LIMNOLOGY
and
OCEANOGRAPHY

ASLO

Limnol. Oceanogr. 00, 2015, 00–00

doi: 10.1002/lno.10046

Local dispersion of nonmotile invasive bivalve species by wind-driven lake currents

Andrea B. Hoyer,[1,2] S. Geoffrey Schladow,[4,5] Francisco J. Rueda*[1,3]
[1]Water Research Institute, University of Granada, Granada, Spain
[2]Department of Ecology, University of Granada, Granada, Spain
[3]Department of Civil Engineering, University of Granada, Granada, Spain
[4]Department of Civil and Environmental Engineering, University of California, Davis
[5]Tahoe Environmental Research Center, University of California, Davis

Abstract

Asian clam (*Corbicula fluminea*) is among the most aggressive freshwater invaders worldwide causing major ecological and economic damage. However, the mechanisms leading to the water-borne dispersion of the species within aquatic ecosystems, particularly lakes, is an area where research is at a relatively early stage. A numerical model has been developed to analyze and describe the dispersion that is produced by the actions of waves and currents. The model represents the basic particle processes of release (R), water-borne transport (T), and survival (S). The model has been applied to a large, deep lake—Lake Tahoe. The dispersion model results reveal that (1) under episodic, extreme wind forcing, larvae are carried away from the original areas, along a discrete number of preferred pathways, (2) bays can act as retention zones, with low current velocities and recirculating eddies, and (3) the majority of the larvae released in the infested areas stay within these areas or disperse on a small spatial scale.

The spread of aquatic invasive species is one of the major ecological and economic threats to lakes and waterways worldwide (Wilcove et al. 1998; Pimentel et al. 2005). In the United States alone, there are about 50,000 invasive species established that cause economic losses estimated at more than $120 billion per year (Pimentel et al. 2005). Invasive species may cause dramatic changes in the ecosystems through perturbations to the interspecific competition, predator–prey interactions, food web structure, nutrient dynamics, hydrologic cycle, and sedimentation rates. Those changes typically lead to the displacement of native species from their natural habitats. The pressure posed by invasive species on native organisms is of such magnitude that their introduction has been ranked second only to habitat loss in the factors that threaten native biodiversity at the global scale (Wilcove et al. 1998). The development of management guidelines for early detection and eradication appears as the primary tool to maintain the ecological integrity of uninvaded habitats (Vander Zanden and Olden 2008). But these guidelines need to be grounded on the sound understanding of the mechanisms by which invasive species spread and colonize new habitats. Such understanding, however, still remains incomplete due to the complex interactions among nonindigenous and indigenous species, humans, and local environmental conditions (Moles et al. 2008).

*Correspondence: fjrueda@ugr.es

Several modeling approaches have been proposed in the literature to represent the dispersion of aquatic invasive species. Most approaches, although, have focused on the analysis of dispersion between aquatic ecosystems conceptualized as "islands" isolated by extended areas of nonsuitable terrestrial habitats (Figuerola and Green 2002). Dispersion in this case is largely mediated by human activities (Green and Figuerola 2005). For example, the pattern of recreational boating traffic between inland water bodies has been shown to be a good proxy for the spatial distribution patterns of the aquatic invasive bivalve *Dreissena polymorpha* (zebra mussel) (Buchan and Padilla 1999). Adult mussels and their larvae tend to attach primarily to macrophytes that entangle on boat trailers (Johnson et al. 2001).

Once in a given water body, the local dispersion of the invasive species from colonized to uncolonized areas can be facilitated by natural processes, such as water currents (Prezant and Chalermwat 1984; Forrest et al. 2012). Mixing and dispersion of invasive species in a river and a semienclosed harbor have been investigated through recent tracer studies (Carr et al. 2004; Wells et al. 2011; Sun et al. 2013). Similarly, Hrycik et al. (2013) have taken a modeling and measurement approach to this problem in a strongly, tidally forced coastal system. In all these cases, there is either unidirectional flow (albeit reversing for a tidal system) or an enclosed environment. In lakes, however, the flows can have

additional complexities, driven as they are by episodic, variable winds, subject to waves, and with the interactions of boundaries. For these reasons, less is known about the role of currents in the local dispersion of invasive species or other planktonic organisms. This work focuses on the local dispersion of the larval form of an invasive species by wind-driven and wave-driven currents in lakes. Specifically, we address the prediction of the local transport and dispersion patterns and spatial evolution of the invasive bivalve *Corbicula fluminea* (Asian clam) in Lake Tahoe, a large subalpine lake on the crest of the Sierra Nevada mountain range (CA-NV; Fig. 1A). *C. fluminea* was first observed in Lake Tahoe in 2002 in very low numbers (Hackley et al. 2008). Its population has increased now to a level where it is having apparent environmental impacts. Its current known distribution (area $\approx 10^6$ m^2) is patchy along the southeast and south shore of the lake, with the densest population established in Marla Bay (Fig. 1). This distribution is believed to be changing, although, due to *C. fluminea's* rapid growth rate and the presence of abundant suitable habitat existing along the shoreline in Lake Tahoe (Herold et al. 2007).

C. fluminea is among the most aggressive freshwater invaders worldwide (McMahon 1999). Its invasion success is based on its rapid population growth, early sexual maturity and short turn over time rather than on its tolerance to environmental fluctuations (McMahon 2002). The species is sensitive to low oxygen conditions and requires sustained water temperatures of 15–16°C or above for reproduction (McMahon 1999; Sousa et al. 2008; Wittmann et al. 2012). *C. fluminea* generally forms colonies or beds with densities that may exceed 6000 clams m^{-2} (Aldridge and McMahon 1978; Wittmann et al. 2012), preferably in areas of coarse and sandy sediments (Karatayev et al. 2003). *C. fluminea* filters out phytoplankton and other suspended particles in the water column which are also food sources for native filter-feeding organisms. It can use its pedal foot to feed on organic matter in the sediment and competes for food resources with native benthic organisms (Hakenkamp et al. 2005). *C. fluminea* can also affect aquatic ecosystem processes in other ways. Excretion of inorganic nutrients, particularly nitrogen, can stimulate the growth of algae and macrophytes (Sousa et al. 2008). The species is believed to facilitate the introduction of parasites, diseases, and other invasive species (Vaughn and Hakenkamp 2001; Sousa et al. 2008). They have also been shown to facilitate the invasion of zebra or quagga mussel by creating localized high calcium environments, as shells from dead clams leach this potentially limiting element (*see* Hessen et al. 2000, and references therein).

Passive (natural) hydraulic transport by water currents is considered to be the main mechanism for the local dispersal of *C. fluminea* (McMahon 1999). The local dispersion largely occurs during the larval and juvenile stages of their life when, as a result of their low density (total dry weight of 0.1 mg at $\sim$ 200 μm shell length) (Aldridge and McMahon 1978), larvae may remain suspended in the surface mixed layer even under minimal turbulence (McMahon 1999). Larvae are not motile but can travel long distances drifting with water currents. The contribution of currents in the local dispersion of Asian clam, however, is not known. Laboratory studies on the dispersion of *C. fluminea* by water currents have focused on the transport of adults (Prezant and Chalermwat 1984; Williams and McMahon 1989). These studies have been conducted with strong, unidirectional and steady currents, more characteristic of rivers than lakes. In lakes, currents are largely forced by winds, waves and convective processes, and are characterized by lower magnitude as well as a higher temporal and spatial variability.

Our goal is to characterize the transport pathways of young life stages of *C. fluminea* and analyze the development of the clam population in a lake environment. Lake Tahoe (CA-NV) is used as a test case, although the modeling approach may be applied in any aquatic system. The approach embodies a number of consecutive steps. These are the determination of the mechanism of larval entrainment (suspension) into the ambient flow; the transport and dispersion characteristics due to the spatially and temporally varying meteorological conditions, lake stratification, and larval density; the resulting preferred migration pathways; and the exposure to environmental stressors (temperature and light) experienced during the journey.

Methods

Approach

A three-dimensional (3D) Lagrangian, individual-based dispersion model (the larval dispersion model) developed by Hoyer et al. (2014) was used to simulate the dispersion of Asian clams larvae. This model is driven by estimates of the advection and turbulence provided by two external computational models: a wave model STWAVE and a 3D hydrodynamic model, Si3D. Both these latter models have been widely used and validated in other locations (see below). The simulations were conducted for a two-month period in 2008 (the study period), when temperature conditions in the lake are known to favor the release of Asian clam larvae. The wave model was validated against field observations from Lake Tahoe by Reardon et al. (2014). The results of a validation of the hydrodynamic model at Lake Tahoe are presented as an appendix.

Wave and hydrodynamic simulations

Wave conditions and wave-induced bottom shear stresses in Lake Tahoe were simulated using STWAVE, a two-dimensional phase-averaged spectral wave model (Smith et al. 2001; Smith 2007; Massey et al. 2011). As STWAVE is a steady-state model, the changing state of the wave field in the lake is calculated as a sequence of quasi-steady states, calculated every Δt_w seconds (wave time step). Wind conditions are averaged over Δt_w, the magnitude of which should

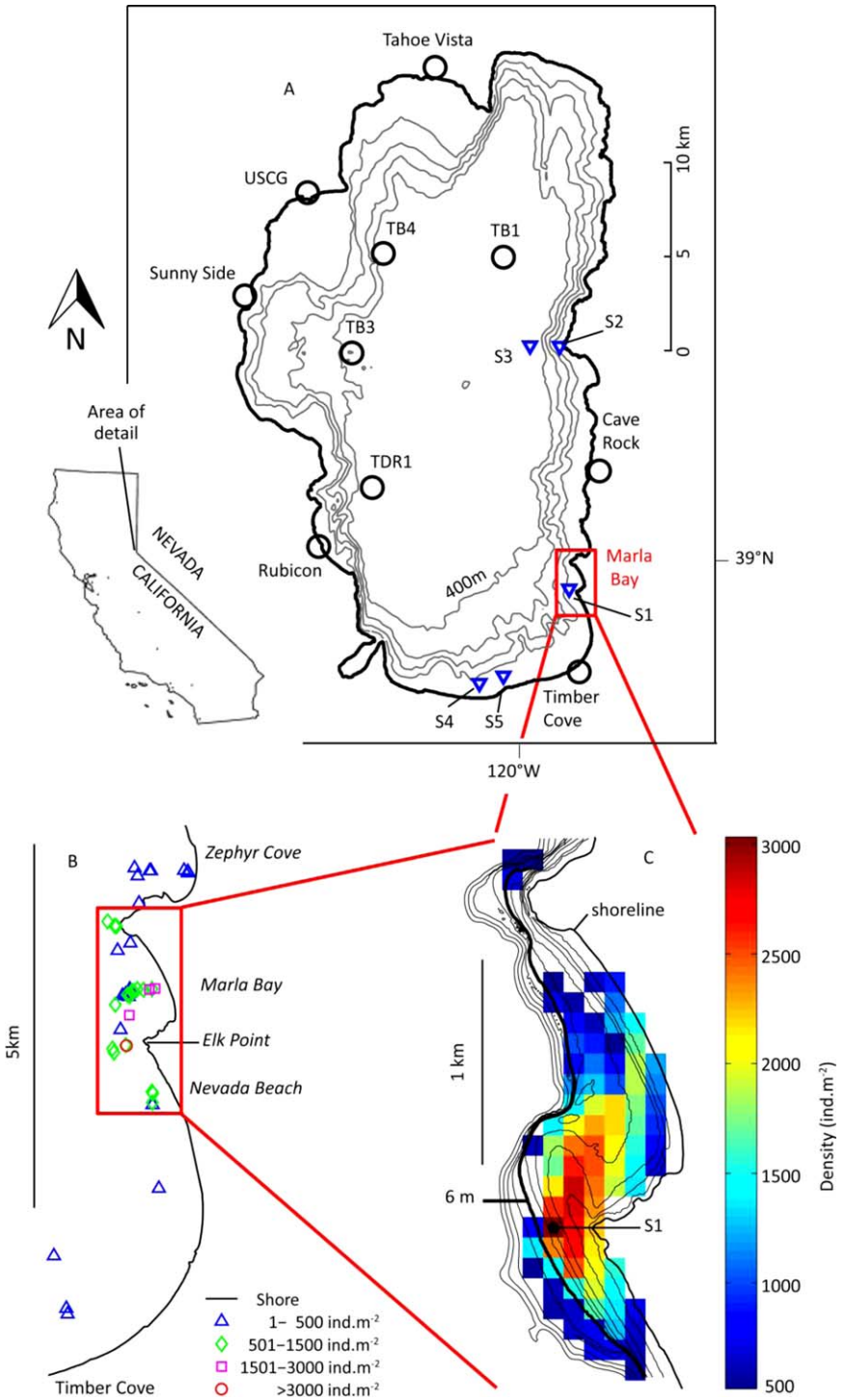

Fig. 1. Lake Tahoe location, bathymetry and location of meteorological stations (dots), initial temperature profile (S3), stations of model output (triangles) and area of interest (A). Density distribution of Asian calm adult population in 2005. Discrete sampling locations (Wittmann et al. 2009) (B) and interpolated map of densities $>$ 500 ind. m^{-2} (C). Black lines mark depth contours (1, 2, 3, 4, 5, 6, 10, 20, 30, and 40 m) for orientation. Six-meter contour marked for reference. S1–S3 mark sampling station for model output. S4 and S5 mark locations of sensors deployment for field observations (*see* text for details).

be longer than the time it takes for the wave field to be generated. The lake currents and diffusivities were computed using a parallel version (Acosta et al. 2010) of the 3D Cartesian hydrodynamic model of Smith (2006). The model solves the 3D form of the shallow water-wave equation and has been extensively validated both against analytical

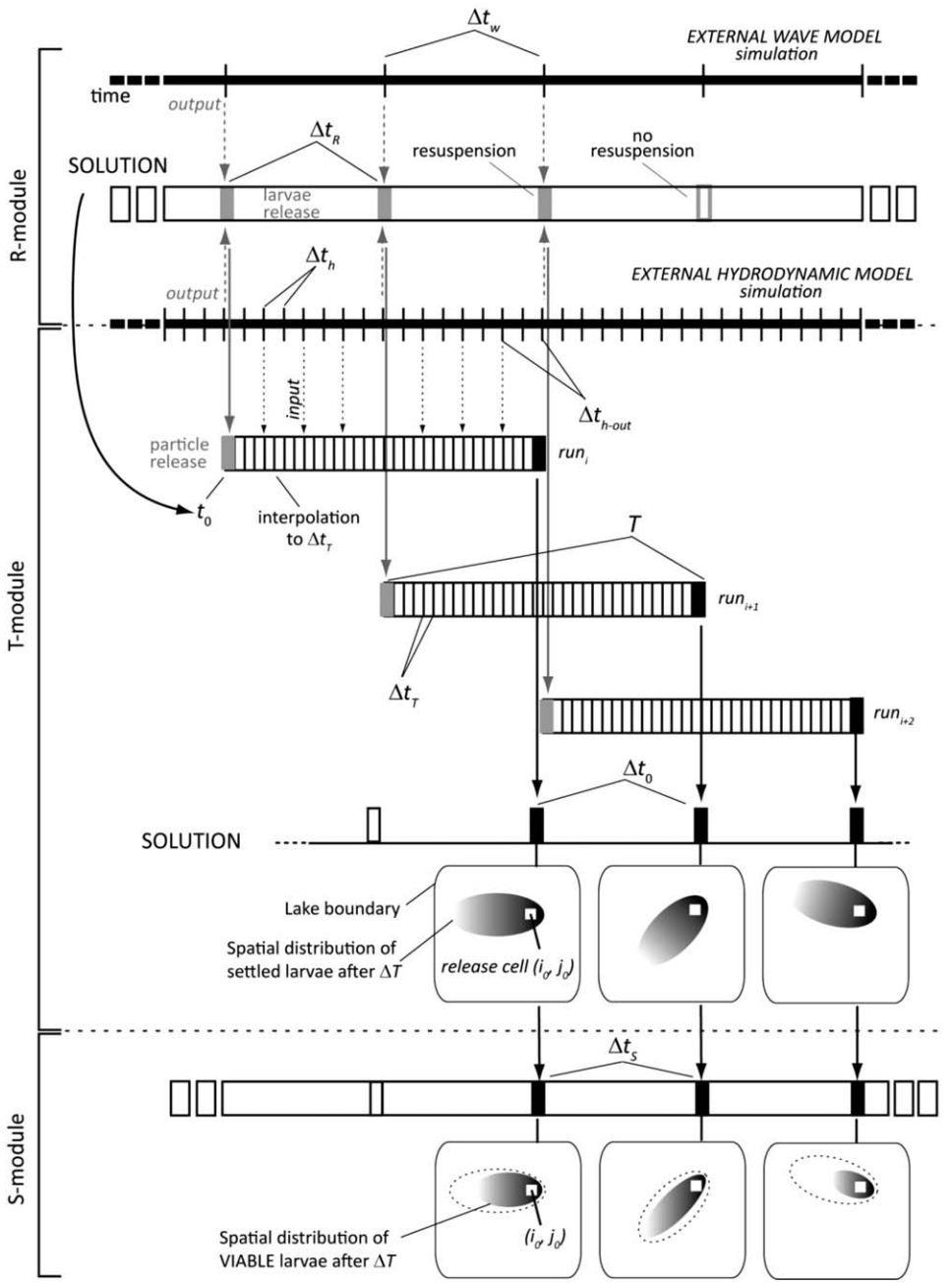

Fig. 2. Flow diagram of the larvae dispersion model. Horizontal lines represent time lines (simulations and runs). Thin vertical bars mark time steps. Module solutions and beginning/end of transport simulations are represented by thick vertical bars. Solid vertical arrows show dependencies between modules. Dashed vertical arrows show output/input dependencies. Shaded ellipses represent model output of final larvae distribution and the indices i_0,j_0 indicate the point of larvae release into the pelagic (*see* text for details).

solutions (Rueda and Schladow 2002; Rueda et al. 2003) and field datasets (Rueda and Schladow 2003; Rueda and Cowen 2005; Rueda et al. 2008). In contrast to the wave model, the transport and mixing model is a truly dynamic model that predicts the changes in the hydrodynamic conditions of the lake every Δt_h seconds (hydrodynamic time step).

To simulate the wave and hydrodynamic conditions in Lake Tahoe, both models were forced using sequences of spatially variable wind fields, constructed through spatial interpolation of ten-minute wind records collected at 10 stations around the lake (Barnes 1964). The models' horizontal grids were 100 m × 100 m. This grid resolution was a compromise between the need to adequately resolve motions within

small embayments and the computational cost. The bathymetry was a modified form of Gardner et al. (1998). The vertical resolution in the hydrodynamic model was variable, ranging from $\Delta z = 0.5$ m at the surface to $\Delta z = 10$ m near the bottom (at a depth of 500 m). The initial temperature profile was obtained from thermistor-chain records (thermistors located at 5, 10, 15, 20, 25, 30, 40, 60, 80, 100, 120, 140, 180, 200, 240, 280, 320, 360, 400, and 440 m depth) at S3 (Fig. 1A) interpolated to the vertical grid spacing. The time step of the hydrodynamic model was $\Delta t_h = 50$ s, primarily based on stability considerations. The horizontal eddy diffusivity K_h was set to 1 m^2 s^{-1}, based on the horizontal grid resolution and the time step (Castanedo and Medina 2002). The wave model was run at $\Delta t_w = 6$ h intervals, a compromise between the time of wave generation, estimated to be O(1)h (Hamilton and Mitchell 1996), and computational cost.

Larval dispersion model

The three different modules of the larval dispersion model are designed to run sequentially and independently of each other (*see* Fig. 2). The model is driven by the output of the wave and hydrodynamic models and run on the same Cartesian grid. The Release module (R-module) represents the growth of larvae in the existing beds and their release into the water column. Release is parameterized using the ratio of shear u^* to settling w_s velocities (Bagnold 1966). The settling velocity is a fixed model parameter, representing the larval size and density. Bottom shear velocities are variable both in space and time and are calculated from wave and hydrodynamic models that have been driven by the measured meteorological data. The output of this module consists of a time series of number of larvae individuals released into the pelagic for every grid cell (i_0, j_0), with a time step of Δt_0 seconds.

The Transport module (T-module) tracks the position and the environmental conditions experienced by larvae in the pelagic after resuspension. The transport simulations are conducted using the 3D time-varying particle tracking model proposed by Rueda et al. (2008). These simulations, in turn, are driven by the 3D time-varying velocity and diffusivity fields produced by the hydrodynamic model. One transport simulation is conducted for every cell (i_0, j_0) of the gridded bottom where the invasive species is known to exist (and reproduce), at every Δt_0 seconds. In each of these simulations, a total of N_0 particles are released from a source cell (i_0, j_0) at time t_0 and tracked during a period ΔT, the time the particles stay in suspension. Once settled, the particles stay at a fixed location and are not able to resuspend again, representing larvae burrowing in the sediments (McMahon and Bogan 2001; Vaughn and Hakenkamp 2001). The solution of this module consists of a spatially varying field of the fraction of the N_0 particles released that have settled after ΔT days on any given grid cell (i, j) and the history of environmental conditions experienced by each individual prior to settling. This solution should be thought of as the response, in terms of the spatial distribution of settled larvae on the lake bottom, to a unit pulse of larvae injected in the water column from cell (i_0, j_0) and at time t_0. Note that the solution is calculated every Δt_0 (Fig. 2).

The Survival module (S-module) accounts for the death/survival of settled larvae subject to the habitat conditions encountered at the site of sedimentation and the transport conditions calculated in the T-module. Individuals reaching a site (i, j) are considered viable if (i) they settle in favorable habitats and (ii) if the environmental conditions endured in transit do not negate their survival. The output of the S-module is a modified version of the spatially variable fields calculated in the T-module and is also calculated every Δt_0 seconds. Here, the fields represent the fraction of viable larvae reaching each site in the lake after a pulse of larvae from a given source cell (i_0, j_0) and at time t_0. From the set of response functions calculated in the T and S modules, together with the results of the R-module through a convolution exercise, one can reconstruct the changes in the spatial distribution of the larval population during the study period. The final larvae distribution is the result of the S-module where the fractions of simulated particles (larvae) that remain viable on settlement in favorable habitats are weighted. The respective weights $\delta_{i_0 j_0}(t_0)$ are obtained from the number of larvae resuspended at cell (i_0, j_0) and at time t_0 divided by the total number of resuspended larvae at the existing clam beds during the study period L_T. A graph showing the links between the different modules and external computations are shown in Figure 2. A more detailed description of this dispersion model can be found in Hoyer et al. (2014).

Application to Lake Tahoe

The larval dispersion model was applied to Lake Tahoe to simulate the dispersion of Asian clam larvae during their release period. Water temperatures of Lake Tahoe are above the minimum value for clam reproduction ($\theta > 15$°C) between the beginning of July and end of September. Denton et al. (2012) observed a lag of four weeks between the time when water temperatures are first suitable for Asian clam reproduction and the time when clams actively reproduce. Therefore, the simulation starts August 1 (day 214), after a month of suitable water temperatures, and lasts for two months, until day 274. Water temperatures above 30°C, lethal for Asian clam and its larvae, were not recorded at Lake Tahoe during the study period. The density distribution of adults in the largest contiguous area of Asian clam identified to date (with clam densities in excess of 500 ind. m^{-2}) is shown in Figure 1C. For the purpose of this study, this area is taken as the only source of larvae in the simulations and is referred to as the existing clam beds.

At the start of the study period, the larvae population was assumed to be zero (i.e., $L(0) = 0$). Clam reproduction was assumed continuous and not bound to a specific time of the

Table 1. Model parameter specification.

Symbol	Parameter	Value/range	Units	Comments/references
tl	Length of study period	2	Month	Reproduction period (Denton et al. 2012)
θ_{min}	Minimal temperature for reproduction	15	°C	McMahon (1999)
θ_{max}	Lethal temperature	30	°C	McMahon (1999)
Δt_R	Time step of release module	6	h	–
Δt_T	Time step of transport module	10	s	Ross and Sharples (2004)
Δt_0	Time between consecutive particle tracking simulations	6	h	–
T	Length of particle tracking simulation	2	d	Kraemer and Galloway (1986)
Δt_S	Time step of survival module	6	h	
μ_g	Larvae growth rate	10	d^{-1}	Denton et al. (2012)
μ_d	Larvae decay rate	0.1	d^{-1}	Jørgensen (1981)
w_s	Larvae settling velocity	10^{-3}	$m\ s^{-1}$	Wildish & Kristmanson (1997), Chandra (pers. comm.)
ρ_w	Water density	10^3	$Kg\ m^{-3}$	–
N_0	Number of released particles	10^4	ind.	–
k_{UV}	Attenuation coefficient of UV radiation	0.15	m^{-1}	Rose et al. (2009)
LD_{50}	Light dose at which 50% of the population dies	5×10^4	Jm^{-2}	Lewis and Whitby (1997), McMahon (pers. comm.)
m	Exponent of light probability function	1.45	–	Lewis and Whitby (1997)
H_{min}	Minimal water column depth	2	m	Wittmann et al. (2009)
H_{max}	Maximal water column depth	39	m	Wittmann et al. (2009)

day so that larvae were free to be released whenever shear conditions were favorable for resuspension of particles from the sediment. The R- and the S-modules were run with a time step equal to Δt_w (i.e., $\Delta t_0 = \Delta t_w = 6$ h). The T-module, in turn, was run with a time step $\Delta t_T = 10$ s, to satisfy the convergence criterion for particle tracking simulations proposed by Ross and Sharples (2004). The transport simulations were driven using velocity and diffusivity fields output every 3600 s ($\Delta t_{h\text{-}output} = 1$ h) from the hydrodynamic model and interpolated to Δt_T. The solar radiation data was also passed to the T-module, every hour, to estimate the environmental conditions affecting the viability of larvae along their trajectories. The number N_0 of particles released in the T-module was set to 10^4. In a series of preliminary experiments, the spatial distribution of larvae after ΔT, expressed as a fraction of released individuals, was invariant for $N_0 > 10^4$. The simulation period of this module, T, is two days, equal to the maximum length of time that Asian calm larvae have been observed to persist in the pelagic (Kraemer and Galloway 1986). The probability of survival and colonization was evaluated based on parameter values reported in the literature. Asian clams are found preferentially on coarse sand beds, which is the most common type of nearshore substrate in Lake Tahoe (Herold et al. 2007). Hence, the lake substrate does not pose any limitation on the potential of colonization. The preferred depths of establishment are set at between 2 m (H_{min}) and 39 m (H_{max}) (Wittmann et al. 2009). The probability of survival was established based on ultraviolet radiation exposure only, given that temperature in Lake Tahoe is always within the acceptable range for Asian clam ($3°C < \theta < 30°C$) (McMahon 1999). The particular values for the model parameters used in the model runs are given in Table 1. Note that some of the kinetic parameter values are specific for Asian clam. Other parameter values were taken from studies conducted on other bivalves, where specific values for Asian clam were not available.

Results

Currents

The depth of the seasonal mixed layer (SML) of Lake Tahoe during the study period was ~ 20 m and the stability of the water column was high, based on the calculated values of the Wedderburn number, W, and the Lake number, L_N, which were both well above unity (Stevens and Imberger 1996). Assuming a two-layer stratification with an upper mixed layer of thickness H, the displacement of the interface, Δh, in response to wind forcing can be estimated as $\Delta h = 0.5\ H/W$ (Shintani et al. 2010). Interface displacement was, therefore, a maximum of 8 m, suggesting that the water column above the 12 m isobath in the existing clam beds at Marla Bay (Fig. 1C) was within the SML. The existing clam beds, hence, were subject primarily to mixing conditions and currents driven directly by winds and wind waves. The basin-scale wind-driven circulation in the SML was generally stable throughout the study period and consisted of three

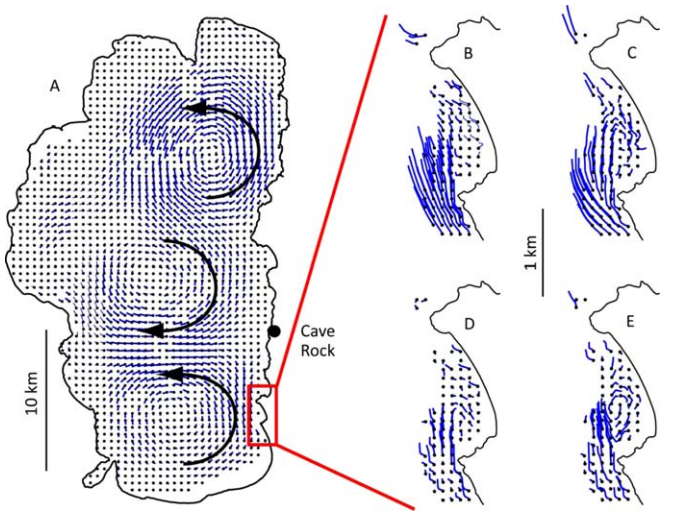

Fig. 3. Circulation patterns in the surface mixed layer at basin-scale (A), at surface (B, C), and bottom (D,E) at the existing clam beds for SE wind (left) and SW wind (right). Streamlines were generated from hourly velocity fields averaged over the study period used as steady-state condition during one hour.

large counter-rotating gyres (Fig. 3A). At the latitude of Marla Bay, the large-scale circulation was convergent producing currents away from the coast.

Currents off Elk Point at the southern end of Marla Bay (Fig. 1B), in the vicinity of the largest clam densities, exhibited changes at both diurnal and synoptic scales in direct response to local winds (Fig. 4A–C). Winds at Marla Bay during the study period were mostly aligned along the NW–SE axis (Fig. 5A) and subject to diurnal changes (Fig. 4A,B). They were typically moderate (< 5 m s^{-1}) from the NW during the afternoon and weak (< 2 m s^{-1}) from the SE at night and early morning. Longshore currents varied in magnitude and direction in response to these diel changes in wind forcing. Currents were southward during the day and northward in the evening. The largest currents were to the north and reached values of O(10^{-1}) m s^{-1} and up to 0.3 m s^{-1} in the evening, shortly after peak NW winds (e.g., day 217; Fig. 4C). These peak northward currents likely occurred as a result of the relaxation of baroclinic pressure gradients set up by the NW winds. These relaxation motions in the evening were in the same direction as the currents associated with the large-scale circulation (Fig. 3A). Cross-shore currents were one order of magnitude lower, alternatively on- and offshore having a zero net displacement (Fig. 4C). The strongest longshore currents occurred on the shallowest nearshore regions, off Elk Point (Fig. 3B,C). By contrast, currents inside Marla Bay were weaker and tended to recirculate, flowing southward inside the bay (Fig. 3B–E). Recirculation within the bay tended to occur during the evening at the times of peak northerly currents off Elk Point, due to flow separation at Elk Point (see below).

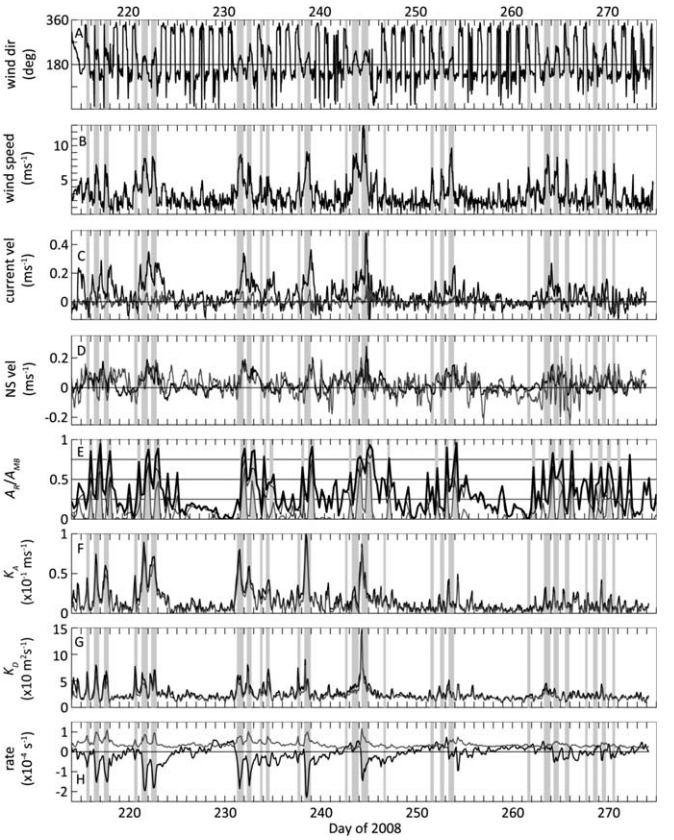

Fig. 4. Temporal variation of wind direction (A); wind speed (B); alongshore (black) and cross-shore (gray) currents at S1 (C); NS current velocities in the coastal-boundary layer at S2 (black) and S3 (gray) (D) (for stations *see* Fig. 1); area where the condition $u^*/w_s > 1$ holds (A_R) as fraction of Marla Bay (A_{MB}) for the wave-induced shear (gray), current-induced shear (thin black) and both wave- and current-driven shear velocities (thick black) (E); advection rate K_A (F) and dispersion rate K_D (G) for neutrally (black) and negatively buoyant (gray) particles; and shear (black) and strain rate (gray) (H). Gray vertical bars mark events were wind direction is 180°–270° and wind speed is > 5 m s^{-1}.

The weak-to-moderate wind regime was disrupted on synoptic scales by strong, episodic forcing events, with SW winds of ~ 10 m s^{-1} occurring with a return period of 7–10 days (Fig. 4A,B). During these SW wind events, currents all along the eastern coast of Lake Tahoe were to the north (Figs. 5D–F, 4C,D). This is particularly evident during the event of day 243–244 (Fig. 4A–D). This northward coastal flow was in the same direction as the currents associated with the southern cyclonic gyre but opposite to the southward basin-scale currents north of Marla Bay (Fig. 3A). Currents off Elk Point reached velocities of up to 0.45 m s^{-1} shortly after peak SW winds (e.g., day 244; Fig. 4C). Within the bay, near-surface water was also forced to flow to the north but more slowly. Once the SW winds ceased, currents inside Marla Bay, with less inertia, decreased more rapidly than those off Elk Point, leading to the formation of a steep velocity gradient and flow separation in the bay (Fig. 3C,E).

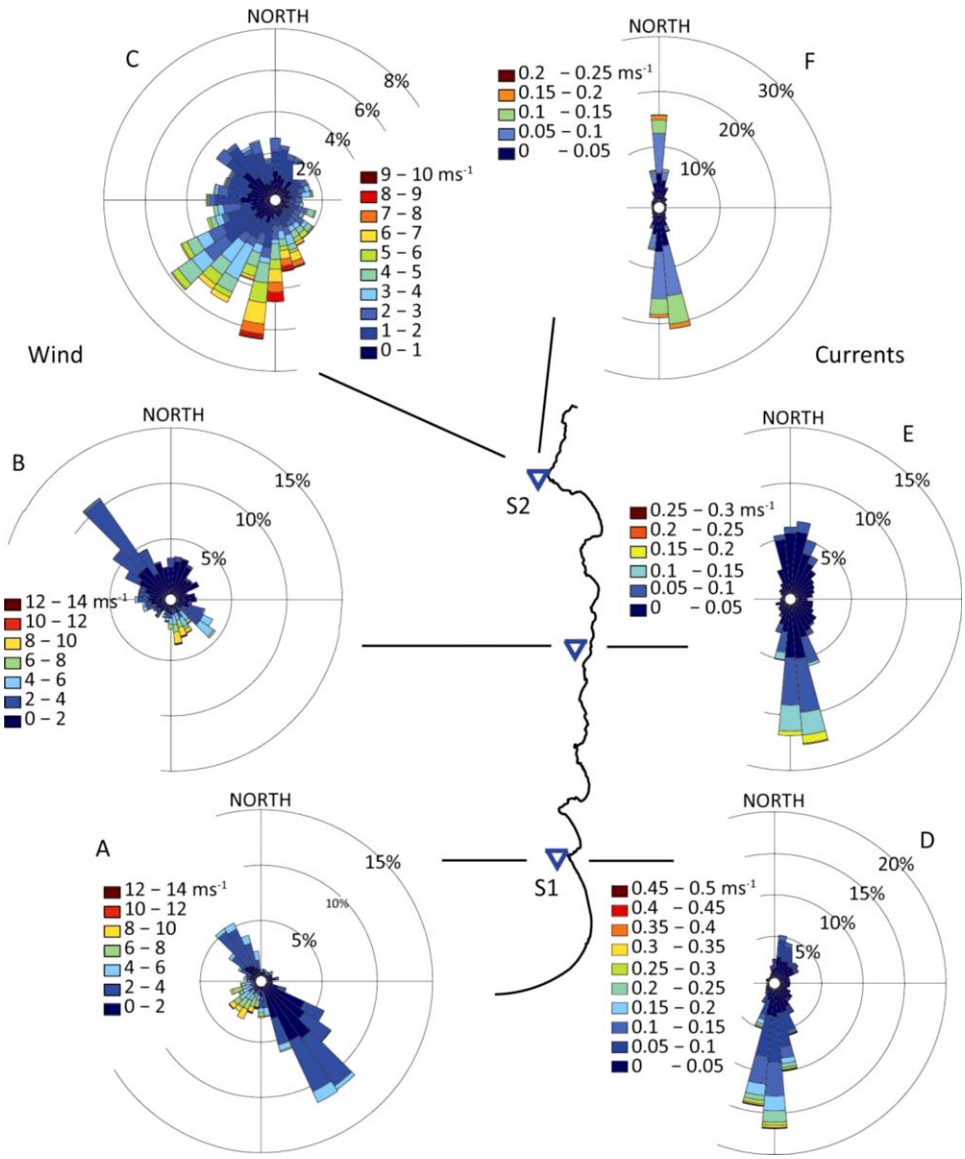

Fig. 5. Wind (left) and current (right) directions and speed along the eastern shore, at S1 (A, D), near Cave Rock (B, E) and at S2 (C, F).

Larval suspension

Suspension of simulated larvae occurred episodically, in response to strong wind forcing events, when the combination of wave orbital velocities and nearshore currents was large enough to entrain and maintain them in the water column. Those events were mainly from the SW and occurred with a return period of about seven days during the study period (Fig. 4A,B). Such strong wind forcing occurred for 17% of the entrainment events but was responsible for 43% of the suspended larvae. The relative contribution of currents and wind waves to bottom shear in Marla Bay, and the fraction of the existing patch contributing larvae into the water column varied in the simulations depending on the exact time and location considered. In general, the broadest resuspension events were episodic, coinciding with the strong SW wind events. During these events turbulence levels were sufficiently energetic ($u^*/w_s > 1$) to induce larval resuspension in over 75% of the existing clam area (Fig. 4E), and the contributions of wave- and current-induced shear stress on the lake bottom tended to be similar. By contrast, under weak-to-moderate wind forcing, bottom shear was dominated by currents (Fig. 4E), and only a small fraction of the patch could be contributing larvae to the water column. As a result of the turbulence at the lake bottom (Fig. 6C), some parts of the existing clam beds could be injecting larvae into the water column almost continuously. The number of larvae released fluctuated as a result of changes in the area with sufficient levels of

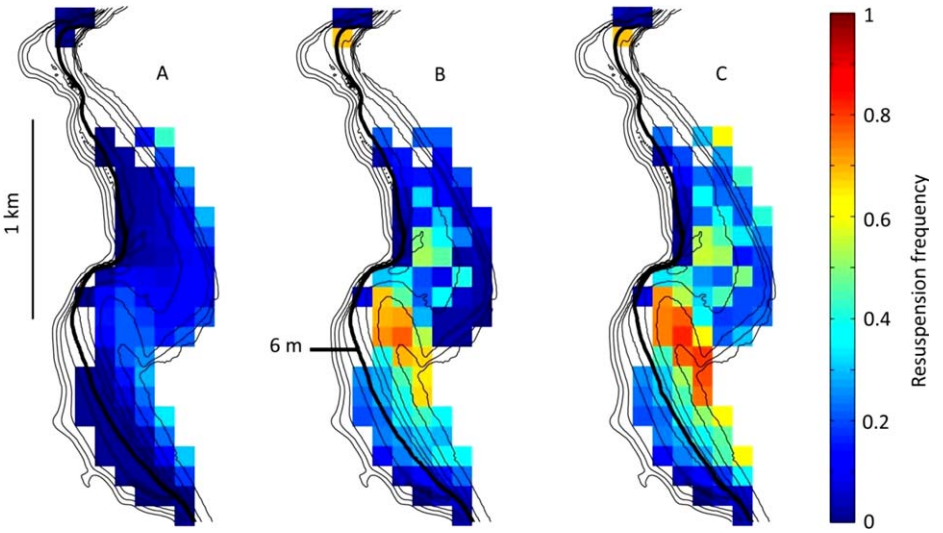

Fig. 6. Horizontal distribution of resuspension frequency in Marla Bay induced by waves (A), currents (B), and combined wave and currents (C). Black lines mark depth contours (1, 2, 3, 4, 5, 6, 10, 20, 30, and 40 m) for orientation. Six-meter contour marked for reference. The frequency of resuspension is estimated at each site as the fraction of time during the study period when the condition $u^*/w_s > 1$ holds.

turbulence to induce resuspension and the number of larvae available for resuspension.

Transport and dispersion

Larval transport and dispersion was also controlled by the nature of the wind events. The greatest transport occurred during the strong SW wind events and after long calm periods. Under weak-to-moderate conditions larvae were suspended but settled within the existing beds, thereby not contributing to the colonization of new areas. A series of simulations were conducted to evaluate advection and dispersion rates of neutrally and negatively buoyant particles from the existing clam beds. A total of 10,000 particles were uniformly seeded in the entire water column above the existing colonies every T_K = 2 h over the study period. The horizontal displacement of the center of mass of the particle cloud D_M provided information about the average cloud velocity V (= D_M $(T_K)^{-1}$). The size and the shape of the cloud calculated at any given time t after the release provided information about the dispersion rates (Peeters et al. 1996). The difference between initial area, A_0 (= 8.9×10^5 m^2, *see* Fig. 1C) and final area of the cloud after two hours of simulation, A_e, was used to estimate an overall dispersion rate K_D as $(A_e - A_0)/T_K$.

For neutrally buoyant particles K_D was O(10) $m^2 s^{-1}$ during most of the study period (Fig. 4G). Dispersion rates were variable during the study period, largely driven by variations in wind forcing. The largest values of K_D, of O(10^2) m^2 s^{-1}, occurred during the strong SW-wind events, when lake currents (Fig. 4C,D), shear and strain rates (Fig. 4H) were maximal. The largest migration rates, quantified in terms of the initial velocity of the cloud (Fig. 4F), also exhibited changes, with the largest values of O(1) m s^{-1} occurring during the episodic SW wind events. At those rates, the cloud could travel up to O(10) km during a period of two hours. These estimates of K_D and V should be considered as upper bounds to the dispersion rates and migration velocities of larvae. First, settling of larvae was not considered. The estimates were, on average, 20% and 28% smaller in the simulations conducted with negatively buoyant particles (with a settling velocity $w_s = 10^{-3}$ ms^{-1}), with differences most pronounced during periods of stronger winds (Fig. 4A,F,G). Second, the area of the initial cloud was always assumed to be that of the existing clam beds and that the larvae occupied the whole water column. This is only true during the events of strong SW winds but not during the periods of weak-to-moderate winds. The dispersion coefficient estimated from experiments conducted with the initial clouds occupying only half the area of the clam beds was approximately 60% of the values shown in Figure 4G. For the initial cloud of particles occupying only the lower half of the water column above the beds, the overall dispersion coefficient reduced by 17%. The dispersion rates of larvae released within Marla Bay was low and larvae resettled at or in the vicinity of their point of suspension. Indeed, 100% of the larvae that were suspended within Marla Bay (near its SE shore) remained within the existing beds. At Elk Point, 20% of the suspended larvae, in turn, were able to leave the existing clam patch.

Pathways of migration

Approximately 16% of the larvae released during the two-month study period were able to leave the existing beds, 77% of which (12% of total) left during periods of strong wind forcing. Nearly 10% of these remained viable and reached favorable habitats. End points, reached by migrating larvae (both successful and unsuccessful) within 48 h after

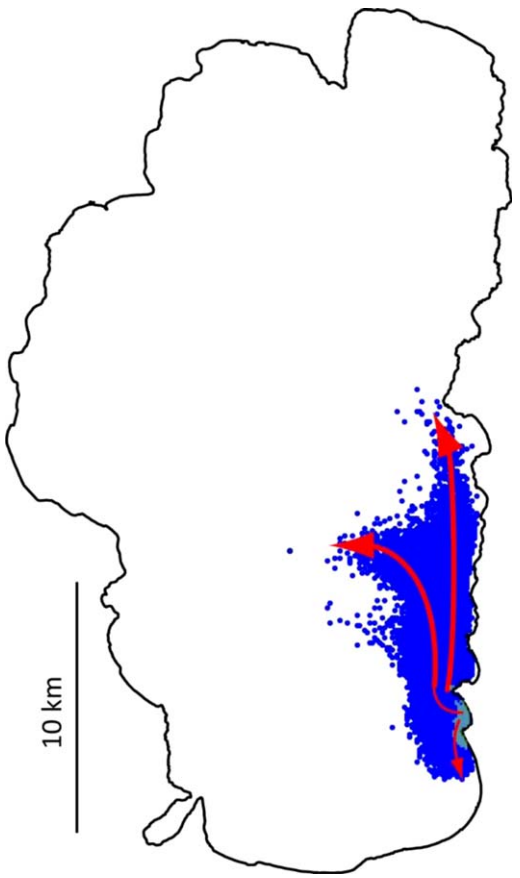

Fig. 7. Final distribution of simulated particles representing Asian clam larvae (*see* text for details). Arrows mark pathways of migration and shaded area marks existing clam beds.

being suspended, are shown in Figure 7. The distribution of these sites suggests the existence of three migration pathways: (1) to the north, along the eastern shoreline of the lake; (2) to the south, along the shoreline; and (3) westward and offshore, following the large-scale circulation. About 50% of the larvae migrating and reaching favorable sites travelled to the North largely during the strong SW events. The remaining travelled to the South. All larvae migrating offshore, 90% of those that dispersed, died due to sedimentation in habitats of depth above the critical value (> 39 m) for Asian clam growth and survival.

The distance travelled along the northward path could be up to 10 km during the strongest SW wind events. Winds during those events were largely uniform over the lake and lead to the development of transport corridors along the coastal-boundary layer. These transport corridors were characterized by strong alongshore currents (*see* Fig. 4C, D) persisting during periods of up to five hours and capable of advecting larvae large distances, while keeping them in suspension. The directionality of the winds during these events largely determined preferential pathway of migration.

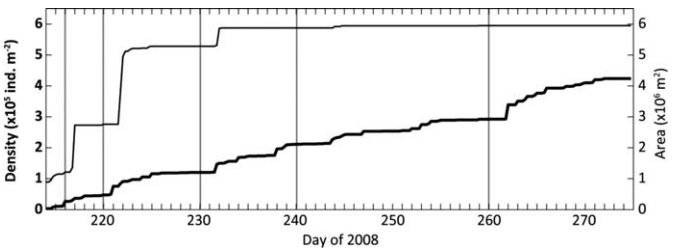

Fig. 8. Fig. 8.Temporal development of simulated Asian clam population (adult and larvae) density at S1 (*see* Fig. 1C) (thick line) and spatial extension (thin line). Note that at the beginning of the study period, the density is equal to the adult density (dens = 3×10^3 ind. m^{-2}) and the area is equal to the area covered by the existing clam population ($A = 8.9 \times 10^5$ m^2). Vertical bars mark instants of time shown in detail in Figure 9.

Velocities were up to 0.5 m s^{-1}, and turbulence levels in the SML were sufficient to keep the larvae in suspension (K_z=10^{-3}–10^{-2} m^2 s^{-1}). Larvae were transported to the south, during periods of weak-to-moderate winds, largely during the afternoon, in response to NW winds. However, the distances travelled along this path were at most 1–2 km. Large migration distances, in general, increased the chances of the population to expand and reach new habitats but also contained a potential risk of mortality. Short migration distances or sedimentation in the existing beds, in turn, enhanced the chances of larval survival. Out of the larvae that settled in vicinity to the existing beds (distance < 1 km) ~ 50% remained viable, compared to < 5% of viable larvae from those that migrated > 1 km.

Evolution of clam population

Almost 84% of the larvae produced in Marla Bay settled over the existing patch, even under extreme wind forcing. Hence, littoral embayments could be potential hot-spots in the process of development and colonization of lakes. Released larvae primarily added to the existing clam population in Marla Bay (Fig. 1C), with large spatial gradients away from the actual beds. The area of the clam population could increase up to 600% (from 8.9×10^5 m^2 to ~ 6×10^6 m^2) during the two-month period (one reproduction period, Fig. 8, 9E). However, these newly colonized sites would have much lower clam densities than what is currently seen in Marla Bay. An increase in spatial extent is consistent with observations of clam individuals north of Marla Bay along the eastern coast up to the latitude of Cave Rock, although there are no quantitative estimates of the exact extent or of the densities (M. E. Wittmann pers. comm.).

Discussion

In the vicinity of the eastern nearshore, flows are mainly directed alongshore, driven by strong, episodic SW winds. Alongshore currents within the coastal-boundary layer have also been reported in other lakes and nearshore coastal

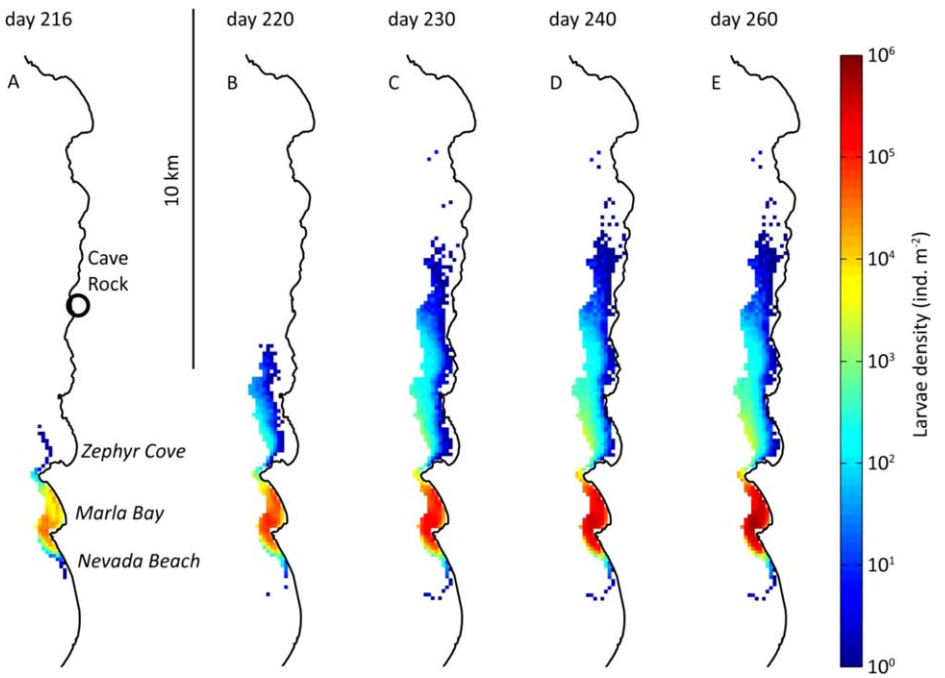

Fig. 9. Simulated larvae distribution on day 216 (A), 220 (B), 230 (C), 240 (D), and 260 (E).

regions (Largier 2003; Rao and Schwab 2007; Nickols et al. 2012). By contrast, flow inside Marla Bay, where Asian clam has established, exhibits recirculating currents. Such eddies are likely the results of flow separation at the bay boundary. Similar observations of separation eddies have been reported in other wind-driven systems (*see* Rueda and Vidal 2009). The formation of recirculating eddies in response to changes in the wind regime has been observed also by Razmi et al. (2013) in an embayment (Vidy Bay) of Lake Geneva. Razmi et al. (2013) found that circulation within the Vidy Bay alternated between alongshore currents and recirculation in function of wind speed and angle.

The lake bottom in nearshore areas is frequently perturbed by wind-waves and wind-driven lake currents, that induce shear above the sediment (Jin and Sun 2007; Chung et al. 2009; Hofmann et al. 2011), and lead to resuspension of sediments and nonattached living organisms (such as larvae). The large contribution of currents to resuspension within the clam beds in Marla Bay (in the range of 2–8 m depth), compared to waves, contrasts with previous publications in which wave-induced shear stress was reported to be the dominant driver of bottom shear in shallow waters (Luettich et al. 1990; Jin and Sun 2007), and even in other nearshore areas of Lake Tahoe (Reardon et al. 2014). Large fluctuations in the number of suspended larvae are driven by the episodic nature of the wind regime. The strength and direction of the wind forcing determines the area with sufficient levels of turbulence to induce resuspension and, thus, the number of larvae available for resuspension. The amount of available larvae at the sediments, in turn, depends on the length of time between wind events inducing suspension and the number of adults present (Hoyer et al. 2014).

Larvae dispersion and migration occurs in form of pulses in response to the episodic nature of the strong wind forcing. The episodic nature of larval migration away from the existing clam beds at Marla Bay is consistent with earlier reports. Coe (1953), for example, found that rare long-distance pulses of larvae dispersal were able to resurge the clam (*Donax gouldi*) population along the Californian coast. MacIsaac et al. (2001) refer to those episodic events of strong impulsive long-distance dispersal as jump dispersal. The dispersion of suspended larvae over the existing population patch is driven predominantly by wind-driven shear and strain deformation rates in the flow field. The initial dispersion rates largely control whether the suspended larvae settle in the area of the existing population patch, travel within the coastal-boundary layer and follow alongshore transport paths, or, if they in turn, move offshore drifting with basin-scale currents. The simulated dispersion rates are one order of magnitude larger than the turbulent diffusion coefficient used in the hydrodynamic simulations but comparable to those reported by others in field-scale numerical experiments (Okely et al. 2010 in Valle de Bravo Reservoir, Mexico). Predicted overall dispersion rates K_D are also large compared to those expected in surface layers of lakes calculated as $K = 3.2 \times 10^{-4}\, l^{1.1}$ (Lawrence et al. 1995) based on a characteristic length scale l ($=A_0^{1/2}$), here taken to represent the initial size of the cloud. This difference can be explained by the high vertical and horizontal shear (Fig. 4H) above the

existing clam beds, due to the proximity of boundaries, compared to the offshore regions of the lake.

Bays that are characterized by low current velocities and recirculation act as traps for suspended benthic larvae. During periods of low physical forcing, the suspended larvae tend to remain within the area of the existing beds, partly as a result of the low displacement rate of the negatively buoyant larvae. However, low dispersion rates also resulted from the predicted recirculation in Marla Bay (see above), which will tend to trap the suspended larvae inside the bay. The trapping effect of bay-scale eddies has been reported in previous studies conducted in large coastal systems. Brooks et al. (1999), for example, showed that eddies forming in Cobscook Bay, Maine, could trap particulates in the side-arms of the estuary. Similar conclusions were obtained by Nishimoto and Washburn (2002), who observed high concentrations of juvenile fish in the center of a large eddy in the Santa Barbara Channel. The trapping effect of shoreline irregularities could favor the preservation of existing population patches at those sites, given that newly produced and trapped larvae can contribute to replenish of the existing population, balancing mortality rates.

In lake systems, the size of the population patch increases in the form of pulses induced by the physical (wind) forcing that drives the dispersal mechanisms of suspension and transport. From the spatial expansion of the patch of newly settled viable larvae A_L (= total extension of larvae patch – extension of existing adult population), we estimate the effective diffusion coefficient K_e as $(A_L)^2\ (T_e)^{-1}$. Here, T_e is the time from the beginning of the reproduction/migration period until the larvae patch has reached its maximal size. The larvae simulations predict an effective diffusivity K_e of O(1) $m^2\ s^{-1}$. This value is within the range of dispersion estimates from diffusion-models found in the literature (Andow et al. 1990). Therefore, the area to be colonized by larvae is limited by the distance larvae can migrate within the time they stay in suspension. High sedimentation rates, thus, decrease the chance of dispersion but increase the chance of survival. Further, the expansion of a population restricted to shallow nearshore areas is bounded by the shore-line on one side and deeper waters on the other side. Offshore transport routes are unfavorable for larval survival, given that they end up on long-transport paths and sedimentation in deep and unsuitable habitats. In this sense, local dispersion of invasive species within a bounded aquatic system differs from unbounded overland dispersion between systems or terrestrial dispersion, where the square root of the population area may increase linearly in time (Skellam 1951). In contrast to sexually reproducing species, asexually reproducing species, such as Asian clam, have no need to find a mate for reproduction. A single propagule may act as a seed for a novel population and, thus, represents a potential risk for the colonization of new habitats. Once the maximal spatial extension is reached, all newly released larvae sediment at previously occupied sites and, thus, add to the pressure exerted on new habitats which will be colonized and will host a new population patch (Lockwood et al. 2005). The final establishment, however, may be jeopardized by environmental and demographic conditions such as characteristics of the receiving microhabitat, food availability, density dependence, or juvenile mortality (Gosselin and Qian 1997; Jerde and Lewis 2007).

Appendix: Validation of the Lake Hydrodynamic and Transport Model

Dataset for lake hydrodynamic model validation

The basin-scale motions and the local current conditions predicted by the hydrodynamic model were validated against data from two types of measurements. Basin-scale lake motion was characterized with Lagrangian drifters (Table 2). Three Lagrangian drifters (drogues) were deployed during the summer of 2008 and their GPS positions were recorded at 10 min intervals. The drogue trajectories depicted circulation patterns and were used to determine the scale of circulation, the general direction of the circulation and to estimate surface current velocity magnitudes in Lake Tahoe. The drogues were released on day 219, 2008, centered at a depth of 1 m below the free surface (default) at site S4 (Fig. 1A; *see* Table 2 for exact coordinates). They were retrieved seven days later, on day 226. The drogues were released between 400 m and 500 m from shore and at the same time. The model results used for the validation of the basin-scale motion consisted of three particle trajectories. The particle tracking model (Hoyer et al. 2014) released 10,000 particles at S4 (Fig. 1A) and tracked their motion with the horizontal velocity field obtained from the hydrodynamic simulations (*see* Wave- and hydrodynamic simulations). As the real drogues are constrained to travel at a constant depth, the depth of the particles was similarly kept constant.

Local current measurements in the nearshore environment in Lake Tahoe were collected using a Nortek Acoustic Doppler Wave and Current Profiler (AWAC). The profiler was moored at N38.94281°, W120.01964° at $\sim$ 5 m depth directed upward to record current velocity and direction from the lake bottom to the surface (except for a blanking distance of $\sim$ 1 m) every 10 min. The current measurements extended from day 204 to day 247 in 2008. A simulated time series of horizontal velocities was output at the grid cell closest to S5 to validate against the AWAC velocity measurements.

Basin-scale circulation

The known circulation pattern of Lake Tahoe in the pelagic generally comprises three counter-rotating gyres: (i) a cyclonic gyre in the south, (ii) an anticyclonic gyre in the center, and (iii) a cyclonic gyre in the north of the basin (Steissberg et al. 2005). These gyres are highly variable in both their size and their positions, being influenced by the diurnal wind field and the variable wind direction over the

Table 2. Instruments deployed for circulation and currents measurements.

Instrument	Location	Coordinates	Time period
Drogue 1	S4	758110, 4314200	219-226, 2008
Drogue 2	S4	758110, 4314600	219-226, 2008
Drogue 3	S4	758110, 4314200	219-226, 2008
Nortek AWAC	S5	N38.94281°, W120.01964°	204-247, 2008

lake (*see* Fig. 5). Within the littoral zone less is known, and these drogue measurements were the first to explore connections between littoral motions and the pelagic motions. The results are shown in Figures 10A, B and C. The black lines represent the measured drogue trajectories and the grey lines are the simulated trajectories. At the outset, the drogues were initially very close together (within one or two grid cells) within the littoral zone. Despite this initial proximity, across the duration of the experiment the drogues trajectories took very different paths. Seemingly, small differences in the initial location made very large differences to the trajectories followed. These differences are in part explainable by the random nature of the forcing but also by the location of the drogues in the interface region between the littoral and pelagic. As is evident in Figure 3, in this area of the lake there are regions of velocity shear and even flow reversals close to shore, and the notion of the trajectories of two drogues diverging in this region is easily understood.

For the simulated drogue trajectories all the same caveats apply but with one major additional one. While the real drogues were driven by currents induced by the actual wind field, the simulations used an approximation to the spatial wind field, derived from an interpolation between 10 wind stations on and around the lake. Spatial and temporal changes in the wind field would be damped out. Thus, the forcing experienced in the simulation is different. Given that the trajectories of the three real drogues displayed great separation despite their initial proximity, it was realized the expectation of close agreement between real and simulated over a weeklong period was unrealistic. While the currents experienced at a point may be close, the integrated effect over a weeklong period would likely produce large departures. Therefore, the goal of the validation was not to try and seek a match between the real and the simulated trajectories—that would be an extremely onerous task in a complex wind field of a high mountain lake. Rather it was to ensure that the scale and directionality of the motions were consistent.

The real drogues all tracked to the north-east initially, following the lake bathymetry. However, their paths diverged after the first 24–36 h. Drogue 1 (Fig. 10A) moved toward Marla Bay (the area of highest *C. fluminea* density; Fig. 1) and appeared to remain trapped by the secondary recirculation in that vicinity, before moving to the southwest as part of the lowest cyclonic gyre. Drogues 2 and 3 (Figure 10B, C) both initially travelled toward the northeast but then took an unexpected turn across the lake toward the west. Drogue 2 eventually became entrained in a northward jet up the west shore before being entrained into the northern-most cyclonic gyre. Drogue 3 ran aground on the west shore before the end of the experiment.

The particles actually agreed quite well with the drogues for the first 36–48 h, moving in the same direction and at about the same speed. During this time they were close to a meteorological station (Timber Cove) so the effect of wind interpolation would have been minimized. However, beyond this point the particles and the drogues parted ways. However, there were two important characteristics that were preserved. First, the particles and drogues that arrived in the vicinity of Marla Bay, all appeared to get trapped there by small scale recirculating currents. Second, at some stage the drogues and the particles all moved rapidly across the lake to the west and were caught up in the large-scale pelagic circulation of the lake.

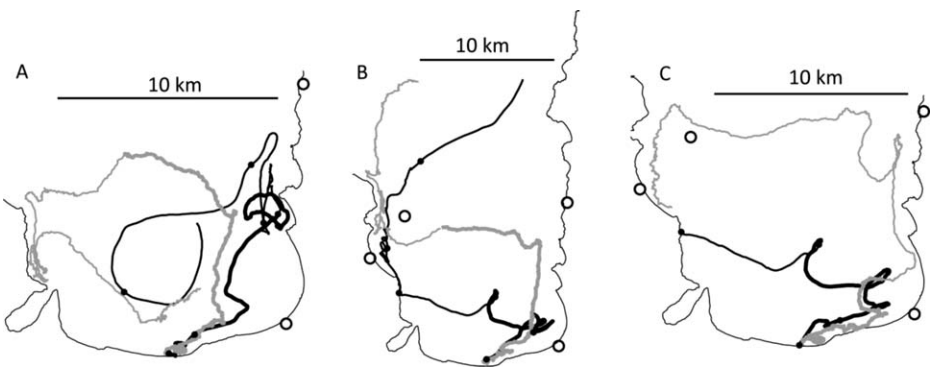

Fig. 10. Observed drogue trajectories (black) and simulated particle trajectories (gray) for Drogue 1 (A), Drogue 2 (B), and Drogue 3 (C). Thick lines mark day 220-213, black dots mark daily intervals, and black circles mark location of meteorological stations (*see* Fig. 1).

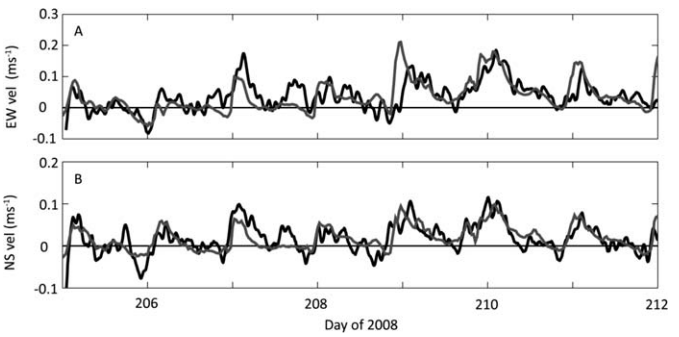

Fig. 11. Observed (black) and simulated (gray) surface current velocities in EW (A) and NS (B) direction at S5 (Fig. 1A).

This validation exercise demonstrated that for the first 2–3 days, the particles and the drogues actually tracked reasonably well. Beyond that time, and especially as the particles moved further away from the shoreline, the trajectories departed, although the general characteristics were preserved. As the present purpose of the model is to track the motion of larvae for just 48 h, we believe that the performance of the model is satisfactory.

Local-scale validation

The hydrodynamic model reproduced the pattern and magnitude of local-scale surface current recorded by the AWAC at S5 (Fig. 1A) reasonably well. These currents were most intense in EW direction (alongshore) with daily maxima in the evening (Fig. 11). Currents in the NS direction were of slightly lower magnitude (Fig. 11B). The current direction was predominantly toward the northeast, consistent with the winds blowing from the south-west recorded at Timber Cove (not shown, but *see* interpolated records for Marla Bay; Fig. 4A). Short-term changes and oscillations were revealed well by the model, for example, between day 208 and 209. The model was also able to reproduce correctly the magnitude of the current. The overall root mean square error was 4.53×10^{-2} m s^{-1} and 2.78×10^{-2} m s^{-1} for the EW and NS velocity, respectively. These error values represent a good match and are comparable with other values reported in the literature. For example, Jin et al. (2000) reported error from 1.52 to 4.76 $\times$ 10^{-2} ms^{-1}. Similarly, Rueda and Schladow (2003) found errors between velocity measurements and model results of 2–5 $\times$ 10^{-2} ms^{-1}.

References

Acosta, M. C., M. Anguita, F. J. Rueda, and F. J. Fernández-Baldomero. 2010. Parallel Implementation of a Semi-Implicit 3-D Lake Hydrodynamic Model. Proceedings of the 2010 International Conference on Computer and Mathematics. Methods in Science and Engineering. (CMMSE) IV: 1026–1037. Available from gsii.usal.es/~CMMSE/images/stories/congreso/volumen2_10.pdf. Accessed January 23, 2014.

Aldridge, D., and R. F. McMahon. 1978. Growth, fecundity, and bioenergetics in a natural population of the Asiatic freshwater clam, *Corbicula Malinensis Phillippi*, from North Central Texas. J. Molluscan Stud. **44**: 49–70.

Andow, D., P. M. Kareiva, S. A. Levin, and A. Okubo. 1990. Spread of invading organisms. Landsc. Ecol. **4**: 177–188. doi:10.1007/BF00132860

Bagnold, R. A. 1966. An approach to the sediment transport problem from general physics. U.S. Geological Survey Professional Paper. 422–I.

Barnes, S. L. 1964. A technique for maximizing details in numerical weather map analysis. J. Appl. Meteorol. **3**: 396–409. doi:10.1175/1520-0450(1964)003<0396:ATFMDI>2.0.CO;2

Brooks, D. A., M. W. Baca, and Y.-T. Lo. 1999. Tidal circulation and residence time in a macrotidal estuary: Cobscook Bay, Maine. Estuar. Coast. Shelf Sci. **49**: 647–665. doi:10.1006/ecss.1999.0544

Buchan, L. A., and D. K. Padilla. 1999. Estimating the probability of long-distance overland dispersal of invading aquatic species. Ecol. Appl. **9**: 254–265. doi:10.1890/1051-0761(1999)009[0254:ETPOLD]2.0.CO;2

Carr, M. L., C. R. Rehmann, J. A. Stoeckel, D. K. Padilla, and D.W. Schneider. 2004 Measurements and consequences of retention in a side embayment in a tidal river. J. Mar. Syst. **49**: 41–53. doi:10.1016/j.jmarsys.2003.05.004

Castanedo, S., and R. Medina. 2002. Análisis de los modelos 3D para la simulación de flujo en aguas de transición. Ing. Agua **9**: 467–481. doi:10.4995/ia.2002.2628

Chung, E. G., F. A. Bombardelli, and S. G. Schladow. 2009. Sediment resuspension in a shallow lake. Water Resour. Res. **45**: W05422. doi:10.1029/2007WR006585

Coe, W. R. 1953. Resurgent populations of littoral marine invertebrates and their dependence on ocean andtidal currents. Ecology **34**: 225–229. doi:10.2307/1930330

Denton, M. E., S. Chandra, M. E. Wittmann, J. Reuter, and J. G. Baguley. 2012. Reproduction and population structure of *Corbicula fluminea* in an oligotrophic subalpine lake. J. Shellfish Res. **31**: 145–152. doi:10.2983/035.031.0118

Figuerola, J., and A. J. Green. 2002. Dispersal of aquatic organisms by waterbirds: A review of past research and priorities for future studies. Freshw. Biol. **47**: 483–494. doi:10.1046/j.1365-2427.2002.00829.x

Forrest, A., and others. 2012. Quantitative assessment of invasive species in lacustrine environments through benthic imagery analysis. Limnol. Oceanogr. **10**: 65–74. doi:10.4319/lom.2012.10.65

Gardner, J. V., L. A. Mayer, and J. E. Hudges Clark. 1998. Cruise Report, RV Inland Surveyor Cruise IS-98: The bathymetry of Lake Tahoe, California-Nevada: U.S. Geological Survey Open-File Report **98–509**, 28 p. Available from http://blt.wr.usgs.gov. Accessed January 23, 2014.

Green, A. J., and J. Figuerola. 2005. Recent advances in the study of long-distance dispersal of aquatic invertebrates

via birds. Divers. Distributions **11**: 149–156. doi:10.1111/j.1366-9516.2005.00147.x

Hackley, S., B. C. Allen, S. G. Schladow, J. E. Reuter, S. Chandra, and M. E. Wittmann. 2008. Lake Tahoe aquatic invasive species incident report: Notes on visual observations of clams in Lake Tahoe and on the beaches along the southeast shore—Zephyr Cove to Timber Cove Marina: April 25, 2008. UC Davis Tahoe Environmental Research Center. Available from http://www.terc.ucdavis.edu/research/CorbiculaIncidentReport_05_07_08.pdf. Accessed November 29, 2013.

Hakenkamp, C. C., S. G. Ribblett, M. A. Palmer, C. M. Swan, J. W. Reid, and M.R. Goodison. 2005. The impact of an introduced bivalve (*Corbicula fluminea*) on the benthos of a sandy stream. Freshw. Biol. **4**: 491–501. doi:10.1046/j.1365-2427.2001.00700.x

Hamilton, D. P., and S. F. Mitchell. 1996. An empirical model for sediment resuspension in shallow lakes. Hydrobiologia **317**: 209–220. doi:10.1007/BF00036471

Herold, M., M. Metz, and J. S. Romsos. 2007. Inferring littoral substrates, fish habitats, and fish dynamics of Lake Tahoe using IKONOS data. Can. J. Remote Sens. **33**: 445–456. doi:10.5589/m07-045

Hessen, D. O., N. E. Alstad, and L. Skardal. 2000. Calcium limitation in *Daphnia magna*. J. of Plankton Res. **22**: 553–568. doi:10.1093/plankt/22.3.553

Hofmann, H., A. Lorke, and F. Peeters. 2011. Wind and ship wave-induced resuspension in the littoral zone of a large lake. Water Resour. Res. **47**: W09505. doi:10.1029/2010WR010012

Hoyer, A. B., M. E. Wittmann, S. Chandra, S. G. Schladow, and F. J. Rueda. 2014. A 3D individual-based aquatic transport model for the assessment of the potential dispersal of planktonic larvae of an invasive bivalve. J. Environ. Manag. **145**: 330–340. doi:10.1016/j.jenvman.2014.05.011

Hrycik, J. M., J. Chassé, B. R. Ruddick, and C. T. Taggart. 2013. Dispersal kernel estimation: A comparison of empirical and modelled particle dispersion in a coastal marine system. Estuar. Coast. Shelf Sci. **133**: 11–22. doi:10.1016/j.ecss.2013.06.023

Jerde, C. L., and M. A. Lewis. 2007. Waiting for invasions: A frame work for the arrival of nonindigenous species. Am. Nat. **170**: 1–9. doi:10.1086/518179

Jin, K.-R., J. H. Hamrick, and T. Tisdale. 2000. Application of three-dimensional hydrodynamic model for Lake Okeechobee. J. Hydraul. Eng. **126**: 758–771. doi:10.1061/(ASCE)0733-9429(2000)126:10(758)

Jin, K.-R., and D. Sun. 2007. Sediment resuspension and hydrodynamics in Lake Okeechobee during the late summer. J. Eng. Mech. **133**: 899–910. doi:10.1061/(ASCE)0733-9399(2007)133:8(899)

Johnson, L. E., A. Ricciardi, and J. T. Carlton. 2001. Overland dispersal of aquatic invasive species: A risk assessment of transient recreational boating. Ecol. Appl. **11**: 1789–1799. doi:10.2307/3061096

Jørgensen, C. 1981. Mortality, growth, and grazing impact of a cohort of bivalve larvae, Mytilus edulis L. Mortality **20**: 185–192. doi:10.1080/00785236.1981.10426570

Karatayev, A. Y., L. E. Burlakova, T. Kesterson, and D. K. Padilla. 2003. Dominance of the Asiatic clam, *Corbicula fluminea* (Müller), in the benthic community of a reservoir. J. Shellfish Res. **22**: 487–493.

Kraemer, L. R., and M. L. Galloway. 1986. Larvae development of Corbicula-Fluminea (Muller) (Bivalvia, Corbiculacea)—An appraisal of its heterochrony. Am. Malacol. Bull. **4**: 61–79.

Largier, J. 2003. Considerations in estimating larval dispersal distances from oceanographic data. Ecol. Appl. **13**: S71–S89. doi:10.1890/1051-0761(2003)013[0071:CIELDD]2.0.CO;2

Lawrence, G. A., K. I. Ashley, N. Yonemitsu, and J. R. Ellis. 1995. Natural dispersion in a small lake. Limnol. Oceanogr. **40**: 1519–1526. doi:10.4319/lo.1995.40.8.1519

Lewis, D., and G. E. Whitby. 1997. Methods and apparatus for controlling zebra and related mussels using ultraviolet radiation. U.S. Patent No.5655483.

Luettich, R. A., D. R. Harlemann, and L. Somlyody. 1990. Dynamic behavior of suspended sediment concentration in a shallow lake perturbed by episodic wind events. Limnol. Oceanogr. **35**: 1050–1067. doi:10.4319/lo.1990.35.5.1050

MacIsaac, H., I. Grigorovich, and A. Ricciardi. 2001. Reassessment of species invasions concepts: The great lakes basin as a model. Biol. Invasions **3**: 405–416. doi:10.1023/A:1015854606465

Massey, T. C., M. E. Anderson, J. McKee Smith, J. Gomez, and R. Jones. 2011. STWAVE: Steady-State Spectral Wave Model User's Manual for STWAVE, Version 6.0. ERDC/CHL SR-11-1. US Army Corps of Engineers, Engineer Research and Development Center, Vicksburg, MS.

McMahon, R. F. 1999. Invasive characteristic of the freshwater bivalve *Corbicula fluminea*, p. 315–345. In Nonindigenous freshwater organisms: Vector, biology, and impacts. CRC Press LLC.

McMahon, R. F. 2002. Evolutionary and physiological adaptations of aquatic invasive animals: R selection versus resistance. Can. J. Fish. Aquat. Sci. **59**: 1235–1244. doi:10.1139/f02-105

McMahon, R. F., and A. E. Bogan. 2001. Mollusca: Bivalvia. p. 331–429. In J. H. Thorp and A. P. Covich [eds.], Ecology and classification of North American freshwater invertebrates. Academic Press.

Moles, A. T., M. A. M. Gruber, and S. P. Bonser. 2008. A new framework for predicting invasive plant species. J. Ecol. **96**: 13–17. doi:10.1111/j.1365-2745.2007.01332.x

Nickols, K. J., B. Gaylord, and J. L. Largier. 2012. The coastal boundary layer: Predictable current structure decreases

alongshore transport and alters scales of dispersal. Mar. Ecol. Prog. Ser. **464**: 17–35. doi:10.3354/meps09875

Nishimoto, M. M., and L. Washburn. 2002. Patterns of coastal eddy circulation and abundance of pelagic juvenile fish in the Santa Barbara Channel, California, USA. Mar. Ecol. Prog. Ser. **241**: 183–199. doi:10.3354/meps241183

Okely, P., J. Imberger, and K. Shimizu. 2010. Particle dispersal due to interplay of motions in the surface mixed layer of a small reservoir. Limnol. Oceangr. **55**: 589–603. doi:10.4319/lo.2009.55.2.0589

Peeters, F., A. Wüest, G. Piepke, and D.M. Imboden. 1996. Horizontal mixing in lakes. J. Geophys. Res. **101**: 18361–18375. doi:10.1029/96JC01145

Pimentel, D., R. Zuniga, and D. Morrison. 2005. Update on the environmental and economic costs associated with alian-invasive species in the United States. Ecol. Econ. **52**: 273–288. doi:10.1016/j.ecolecon.2004.10.002

Prezant, R. S., and K. Chalermwat. 1984. Flotation of the bivalve *Corbicula fluminea* as a means of dispersal. Science **225**: 1491–1493. doi:10.1126/science.225.4669.1491

Rao, Y. R., and D. J. Schwab. 2007. Transport and mixing between the coastal and offshore waters in the great lakes: A review. J. Great Lakes Res. **33**: 202–218. doi:10.3394/0380-1330(2007)33[202:TAMBTC]2.0.CO;2

Razmi A. M., D. A. Barry, R. Bakhtyar, N. Le Dantec, A. Dastgheib, U. Lemmin, and A. Wüest. 2013. Current variability in a wide and open lacustrine embayment in Lake Generva (Switzerland). J. Great Lakes Res. **39**: 455–465. doi:10.1016/j.jglr.2013.06.011

Reardon, K. E., P. A. Moreno-Casas, F. A. Bombardelli, F. J. Rueda, and S.G. Schladow. 2014. Wind-driven nearshore sediment resuspension in a deep lake during winter. Water Resour. Res. **50**: 8826–8844. doi:10.1002/2014WR015396

Rose, K. C., C. E. Williamson, S. G. Schladow, M. Winder, and J.T. Oris. 2009. Patterns of spatial and temporal variability of UV transparency in Lake Tahoe, California-Nevada. J. Geophys. Res. **114**: G00D03. doi:10.1029/2008JG000816

Ross, O. N., and J. Sharples. 2004. Recipe for 1-D Lagrangian particle tracking models in space-varying diffusivity. Limnol. Oceanogr. Methods **2**: 289–302. doi:10.4319/lom.2004.2.289

Rueda, F. J., and E. A. Cowen. 2005. Residence time of a freshwater embayment connected to a Large Lake. Limnol. Oceanogr. **50**: 1638–1653. doi:10.4319/lo.2005.50.5.1638

Rueda, F. J., and S. G. Schladow. 2002. Quantitative comparison of models for barotropic response of homogenous basins. J. Hydraul. Eng. **128**: 201–213. doi:10.1061/(ASCE)0733-9429(2002)128:2(201)

Rueda, F. J., and S. G. Schladow. 2003. Dynamics of large polymictic Lake II: Numerical simulations. J. Hydraul. Eng. **129**: 92–101. doi:10.1061/(ASCE)0733-9429(2003)129:2(92)

Rueda, F. J., S. G. Schladow, and J. F. Clark. 2008. Mechanisms of contaminant transport in a multi-basin lake. Ecol. Appl. **18**: A72–A88. doi:10.1890/06-1617.1

Rueda, F. J., S. G. Schladow, and S. O. Pálmarsson. 2003. Basin-scale internal wave dynamics during a winter cooling period in a large lake. J. Geophys. Res. **108**: 3097. doi:10.1029/2001JC000942

Rueda, F. J., and J. Vidal. 2009. Currents in the upper mixed layer and in unstratified water bodies. p. 568–582. In G. E. Likens [ed.]. Encyclopedia of inland water. Elsevier.

Shintani, T., A. de la Fuente, Y. Niño, and J. Imberger. 2010. Generalizations of the Wedderburn number: Parameterizing upwelling in stratified lakes. Limnol. Oceanogr. **55**: 1377–1389. doi:10.4319/lo.2010.55.3.1377

Skellam, J. G. 1951. Random dispersal in theoretical populations. Biometrica **38**: 196–218. doi:10.1093/biomet/38.1-2.196

Smith, J. M. 2007. Full-plane STWAVE with bottom friction: II. Model overview CHETN-I-75. Vicksburg, MS: U.S. Army Engineer Research and Development Center. Available from http://chl.erdc.usace.army.mil/chetn.

Smith, J. M., A. R. Sherlock, and D. T. Resio. 2001. STWAVE: Steady-state spectral wave model user's manual for STWAVE, Version 3.0. No. ERDC/CHL SR-01-1. Engineer Research and Development Center, Vicksburg, MS.

Smith, P. E. 2006. A semi-implicit, three-dimensional model for estuarine circulation. Open-File Report 2006-1004. U.S. Department of the Interior. U.S. Geological Survey.

Sousa, R., C. Antunes, and L. Guilhermino. 2008. Ecology of the invasive Asian clam Corbicula fluminea (Müller, 1774) in aquatic ecosystems: An overview. Ann. Limnol. Int. J. Limnol. **44**: 85–94. doi:10.1051/limn:2008017

Steissberg, T. E., S. J. Hook, and S. G. Schladow. 2005. Measuring surface currents in lakes with high spatial resolution thermal infrared imagery. Geophys. Res. Lett. **23**: L11402. doi:10.1029/2005GL022912

Stevens, C., and J. Imberger. 1996. The initial response of a stratified lake to a surface shear stress. J. Fluid Mech. **312**: 39–66. doi:10.1017/S0022112096001917

Sun, Y., M. G. Wells, S. A. Bailey, and E. J. Anderson. 2013 Physical dispersion and dilution of ballast water discharge in the St. Clair River: Implications for biological invasions. Water Resour. Res. **49**: 2395–2407. doi:10.1002/wrcr.20201

Vander Zanden, M., and J. D. Olden. 2008. A management framework for preventing the secondary spread of aquatic invasive species. Can. J. Fish. Aquat. Sci. **65**: 1512–1522. doi:10.1139/F08-099

Vaughn, C., and C. C. Hakenkamp. 2001. The functional role of burrowing bivalves in freshwater ecosystems. Freshw. Biol. **46**: 1431–1446. doi:10.1046/j.1365-2427.2001.00771.x

Wells, M. G., S. Bailey, and B. Ruddick (2011) The dilution and dispersion of ballast water discharged into Goderich

Harbor. Mar. Pollut. Bull. **62**: 1288–1296. doi:10.1016/j.marpolbul.2011.03.005

Wilcove, D., D. Rothstein, J. Dubow, A. Phillips, and E. Losos. 1998. Quantifying threats to imperiled species in the United States. BioScience **48**: 607–615. doi:10.2307/1313420

Wildish, D., and D. Kristmanson. 1997. Benthic suspension feeders and flow. Cambridge Univ. Press.

Williams, C. J., and R. F. McMahon. 1989. Annual variations of tissue biomass and carbon and nitrogen content in the freshwater bivalve *Corbicula fluminea* relative to downstream dispersal. Can. J. Zool. **67**: 82–90. doi:10.1139/z89-013

Wittmann, M. E., S. Chandra, J. E. Reuter, S. G. Schladow, B. C. Allen, and K. J. Webb. 2012. The control of an invasive bivalve, *Corbicula fluminea*, using gas impermeable benthic barriers in a large natural lake. Environ. Manag. **49**: 1163–1173. doi:10.1007/s00267-012-9850-5

Wittmann, M. E., J. E. Reuter, S. G. Schladow, S. Hackley, B. C. Allen, A. Caires, and S. Chandra. (2009) Asian clam (*Corbicula fluminea*) of Lake Tahoe: Preliminary scientific findings in support of a management plan. UC Davis Tahoe Environmental Research Center. Available from http://www.terc.ucdavis.edu/research/AsianClam2009.pdf.

Acknowledgments

Funding was provided by the US Forest Service under the Southern Nevada Public Lands Management Act (SNPLMA). The parallel version of the hydrodynamic model was developed under the project CGL2008-06101 funded by the Spanish Government (*Ministerio de Innovación y Ciencia de España*). We are grateful to Marion Wittmann, (University of Notre Dame), Todd Steissberg and Kristin Reardon (UC Davis) for providing some of the field data. We would lik\e to thank William Fleenor (UC Davis) and Simon Hook (NASA) for providing the meteorological information. We also thank Oliver Ross (CSIC) for his contribution to the particle tracking model. The first author was supported by a PhD grant (*Formación del Profesorado Universitario*) from the Spanish Government. We are grateful for the insightful comments of the anonymous reviewers.

Submitted 24 January 2014
Revised 2 October 2014
Accepted 30 October 2014

Associate editor: Miki Hondzo